C. R. Chimie 15 (2012) 627–632

Contents lists available at SciVerse ScienceDirect

Comptes Rendus Chimie

www.sciencedirect.com

Full paper/Mémoire

Covalent hydration of nitrobenzofuroxans compounds: Kinetic and theoretical study using reactivity–selectivity descriptor

Malika Mokhtari [a], Nadia Ouddai [b,*], Nadjia Latelli [b,c], Hafida Merouani [b]

[a] Laboratoire de chimie inorganique et environnement, université Abou-Bekr-Belkaid, BP 119, 13000 Tlemcen, Algeria
[b] Laboratoire de chimie des matériaux et des vivants: activité, réactivité, université El-Hadj Lakhdar, Batna, Algeria
[c] Département de chimie, faculté des sciences, université de M'sila, BP 166 Ichbilia, M'sila 28000, Algeria

ARTICLE INFO

Article history:
Received 5 December 2011
Accepted after revision 9 May 2012
Available online 23 June 2012

Keywords:
Nitrobenzofuroxans
Covalent hydration
Conceptual DFT
Reactivity–selectivity descriptor

ABSTRACT

A kinetic study of the covalent hydration of a series of nitrobenzofuroxans, to give the corresponding hydroxy σ-adduct, in aqueous solution is reported. Analysis of the data obtained in the pH range 0.8–13 has allowed dissection of the observed rates into forward ($k_1^{H_2O}$, $k_2^{OH^-}$) and reverse ($k_{-1}^{H^+}$, k_{-2}) rate constants as well as the obtention of pKa values for H_2O addition to the carbocyclic ring. Global and local DFT-based reactivity descriptors are used to rationalize the trends observed in reaction rate constants and to explain the main reaction product experimentally. The reactivity–selectivity dual descriptor has been used to characterize the regio-selectivity that might be driving the covalent hydration reactions.

RÉSUMÉ

Une étude cinétique de l'hydratation covalente d'une série de nitrobenzofuroxanes, pour donner le σ-adduit correspondant, en solution aqueuse a été réalisée. L'analyse des données obtenues sur la gamme de pH 0,8–13 a permis la dissection des constantes de vitesse observées pour la formation des adduits ($k_1^{H_2O}$, $k_2^{OH^-}$) et inverse ($k_{-1}^{H^+}$, k_{-2}) ainsi que l'obtention des valeurs de pKa par addition de H_2O au carbocyclique. Des descripteurs de réactivité globaux et locaux dérivant de la DFT sont utilisés pour rationaliser les tendances observées dans les constantes de vitesse de réaction et d'expliquer le produit de la réaction expérimentalement obtenu. Le descripteur dual de la réactivité–sélectivité a été utilisé pour caractériser la régio-sélectivité qui pourrait être conduite aux réactions d'hydratation covalente.

1. Introduction

A new development in the area of electron-deficient aromatics in the last two decades is the discovery of very powerful electrophilic heteroaromatic structures, such as 4,6-dinitrobenzofuroxan (**DNBF**) [1–8].

The p*K*a for the formation of the hydroxy σ-adduct **1** according to Eq. (1) in Scheme 1 is 3.75 at 25 °C, as compared with a pKa value of 13.43 for formation of the analogous adduct **2** of 1,3,5-trinitrobenzene (TNB), the conventional reference aromatic electrophile in σ-complex chemistry [9]. Extensive studies have revealed that **DNBF** is stronger electrophile than the positively charged 4-nitrobenzenediazonium cation (3) [6].

Recently, Mokhtari et al. kinetically studied the covalent hydration of 4-nitro-6-trifluoromethanesulfonylbenzofuroxan **4a** to give the corresponding hydroxy σ-adduct in aqueous solution. Among the most significant results that they obtained, the discovery which the 4-nitro-6-trifluoromethanesulfonylbenzofuraxan is the most stable hydroxyl σ-adduct to date (pKa = 2.95) and that its even more electrophile that **DNBF** [10].

* Corresponding author.
E-mail address: ouddai_nadia@yahoo.fr (N. Ouddai).

1631-0748/$ – see front matter © 2012 Académie des sciences. Published by Elsevier Masson SAS. All rights reserved.
http://dx.doi.org/10.1016/j.crci.2012.05.008

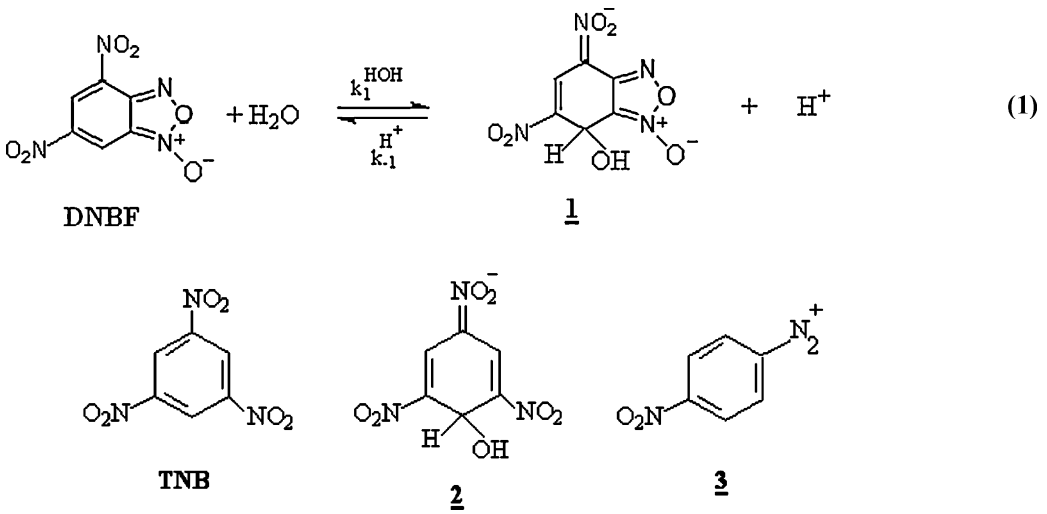

Scheme 1. p*K*a for the formation of the hydroxy σ-adduct **1** of 4,6-dinitrobenzofuroxan **DNBF**, with the adduct **2** of 1,3,5-trinitrobenzene **TNB**.

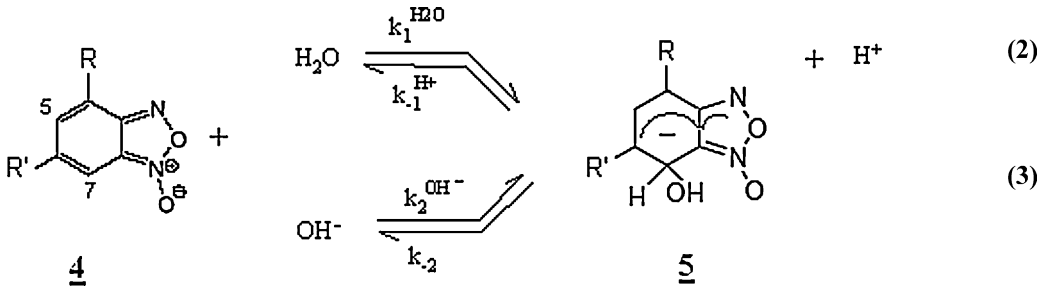

a) R=NO_2; R'=SO_2CF_3

b) R=NO_2; R'=CN

c) R=CN; R'=NO_2

d) R=NO_2; R'=CF_3

e) R=CF_3; R'=NO_2

Scheme 2. Covalent hydration reactions of the 4-(or 6-) nitrobenzofurazans, 4, variously substituted in -6(or -4).

In this article, we report the results of the a kinetic study of the covalent hydration of the 4-(or-6) nitrobenzofuroxans, **4**, variously substituted in 6-(or 4-) by other electron-withdrawing groups such as CF_3, CN, SO_2CF_3 [10] in aqueous solution, to give the adducts **5** according to Scheme 2.

Another objective of this work is to explore how the global and local reactivity of nitrobenzofuroxans can be connected to the change in reaction rates. The goal of this paper is twofold, on one side we want to rationalize the change in the experimental rate constants in terms of descriptors of chemical reactivity of the interacting molecules; then we want to predict the sites on the electrophiles where nucleophile will attack in order to produce the chemical reaction. For this purpose, several reactivity descriptors based on Density Functional Theory (DFT) [11] such as chemical potential, hardness, electrophilicity are calculated and analyzed in the light of the Hard-Soft Acids-Bases (HSAB) [12] principle that defines the conceptual framework that will be used to rationalize the nucleophilic-electrophilic interactions.

2. Results and discussion

2.1. Kinetic and thermodynamic studies

All rates and equilibrium measurements pertaining to Scheme 2 were made at 25 °C and constant ionic strength of 0.2 M maintained with KCl in aqueous solutions. Dilute hydrochloric acid solution, various buffer solutions and dilute potassium hydroxide solution were used to cover a pH range of 0.8–13. All pH values were measured relative

Table 1
Kinetic and thermodynamic parameters for formation and decomposition of hydroxyl σ-adducts in aqueous solution, $T = 25\ ^{\circ}C$, $I = 0.2$ mol.dm^{-3} KCl.

Adducts	pKa	$k_1^{H_2O}(s^{-1})$	$k_{-1}^{H^+}(M^{-1}\ s^{-1})$	$k_2^{OH^-}(M^{-1}\cdot s^{-1})$	$k_{-2}(s^{-1})$
5a[a]	2.95	0.15	100.3	72150	10^{-6}
5b	4.65	10^{-3}	31	1060	10^{-6}
5c	5.86	$2.6\cdot10^{-3}$	3700	2740	$3\cdot10^{-5}$
5d	6.50	$1.5\cdot10^{-5}$	39.6	270	$1.1\cdot10^{-5}$
5e	8.19	$6.3\cdot10^{-5}$	7500	502	10^{-3}
DNBF[b]	3.75	$3.45\cdot10^{-2}$	146	33500	$2.5\cdot10^{-6}$

[a] See reference [10].
[b] See reference [4].

to standard state in pure water accordingly to the relation $[H^+] = 10^{-pH}/\gamma_{\pm}$ holds with $\gamma_{\pm}$ being the mean activity coefficient in 0.2 M KCl ($\gamma_{\pm} = 0.75$ at 25 °C) [13].

2.1.1. pK_a values of 4

Using appropriate buffer solutions (see experimental section), the pK_a values for the σ-complexation of **4** according to Eq. (2) were readily determined from the observed absorbance variations at $\lambda_{max} \approx 345$–425 nm of the resulting adducts **5** obtained at equilibrium as a function of pH. These actually describe a clear acid-base type of equilibrium, as evidenced by the observation of a good straight line with unit slope, fitting Eq. (4). Results obtained are summarized in Table 1.

$$\log \frac{[5]}{[4]} = \text{pH-pKa} \qquad (4)$$

2.1.2. pH rate profiles for covalent hydration of 4

The kinetic studies of formation and decomposition of the adduct **4** according to the two pathways of the Scheme 2 were studied in the pH range 0.8–13 by stopped–flow spectrophotometry. The rate measurements were carried out under pseudo first-order conditions with a substrate or adduct concentration of $3–6 \times 10^{-5}$M. In agreement with the direct equilibrium approach depicted in Scheme 2, only one relaxation time corresponding to the formation ($pH > pK_a$) or decomposition ($pH < pK_a$) of the adducts was observed in all cases were measured at 25 °C and constant ionic strength of 0.2 M maintained with KCl. The variations in the first-order rate constant, k_{obsd}, for the combined formation and decomposition of **5** are plotted in Figs. 1–4 as a function of pH. In the experiments where buffer catalysis was observed, the k_{obsd} values used to draw the pH rate profiles where those extrapolated to zero buffer concentration.

The observed rate constant may be expressed at each pH as the sum of the individual first order rate constant for formation (k_f) and decomposition (k_d) of **5**. Eq. (5). Thus, values of k_f and k_d can be readily derived from k_{obsd} through Eqs. 6 and 7.

$$k_{obsd} = k_f + k_d \qquad (5)$$

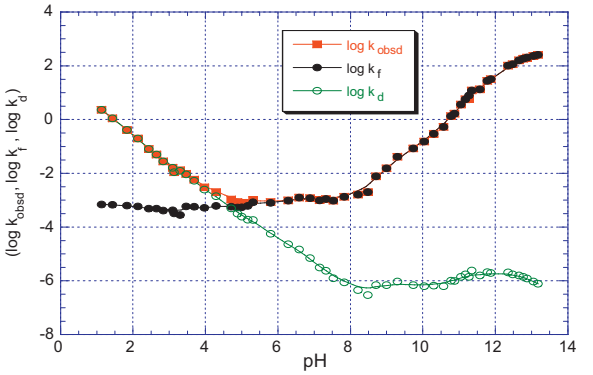

Fig. 1. pH dependence of k_{obsd} (s^{-1}) for the formation and decomposition of the adduct **5b** in aqueous solution; $T = 25\ ^{\circ}C$, $I = 0.2$ mol.dm^{-3} KCl. The (•) and (o) lines refer to the calculated contributions of the k_f and k_d components according to Eqs. (6) and (7).

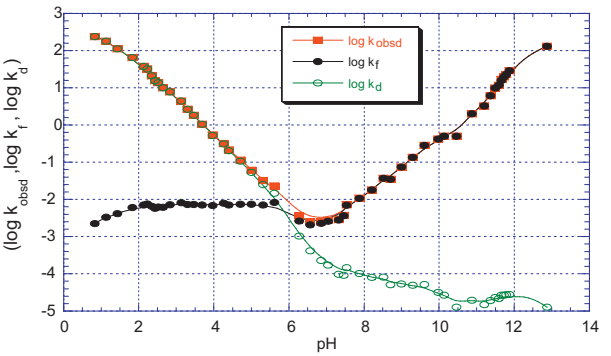

Fig. 2. pH dependence of k_{obsd} (s^{-1}) for the formation and decomposition of the adduct **5c** in aqueous solution; $T = 25\ ^{\circ}C$, $I = 0.2$ mol.dm^{-3} KCl. The (•) and (o) lines refer to the calculated contributions of the k_f and k_d components according to Eqs. (6) and (7).

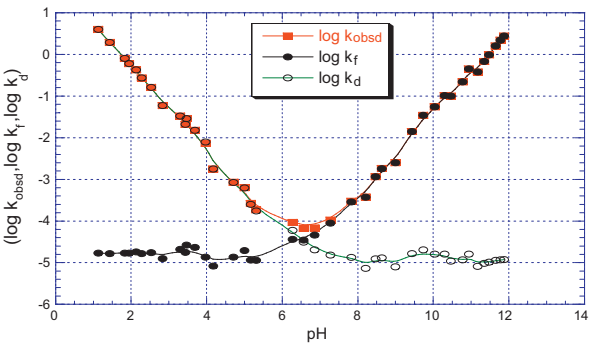

Fig. 3. pH dependence of k_{obsd} (s^{-1}) for the formation and decomposition of the adducts **5d** in aqueous solution; $T = 25\ ^{\circ}C$, $I = 0.2$ mol.dm^{-3} KCl. The (•) and (o) lines refer to the calculated contributions of the k_f and k_d components according to Eqs. (6) and (7).

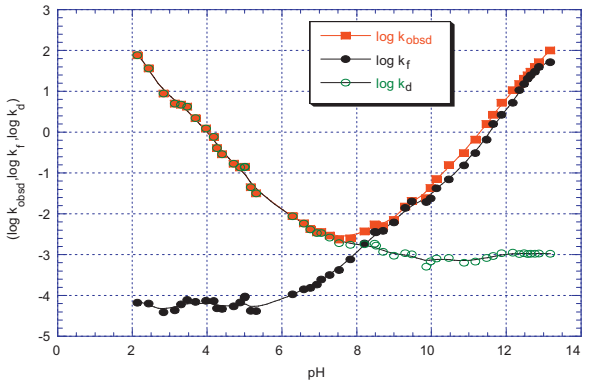

Fig. 4. pH dependence of k_{obsd} (s^{-1}) for the formation and decomposition of the adducts **5e** in aqueous solution; $T = 25$ °C, $I = 0.2$ mol.dm^{-3} KCl. The (•) and (o) lines refer to the calculated contributions of the k_f and k_d components according to Eqs. (6) and (7).

$$k_f = \frac{k_{obsd}}{1 + \frac{10^{-pH}}{10^{-pK_a}}} \tag{6}$$

$$k_d = \frac{k_{obsd}}{1 + \frac{10^{-pK_a}}{10^{-pH}}} \tag{7}$$

The two corresponding pH rate profiles shown in Figures 1–4 are nicely consistent with Eqs. (8) and (9) respectively, in which the rate constants refer to the various individual pathways depicted in Scheme 2.

$$k_f = k_1^{H_2O} + \frac{k_2^{OH^-} K_w}{10^{-pH}\gamma^{\pm}} \tag{8}$$

$$k_d = k_{-2} + \frac{10^{-pH} k_{-1}^{H^+}}{\gamma^{\pm}} \tag{9}$$

Least-square fitting of k_f and k_d to Eqs. (8) and (9) gave the parameters which are collected together with those for relevant systems, in Table 1.

The Table 1 shows that the substitution of one of the two NO_2 groups of the **DNBF** affects very strongly the thermodynamic of σ-complexation, and this in a different way according to whether substitution intervenes in ortho or para position of carbon -7, site of the addition of ion OH^-.

Terrier observed that a para-nitro group plays a dominating role in the stabilization of the negative charge of the σ-adduct [14].

The substitution of group 4-NO_2 by groups CN or CF_3, of which the attractive characters increase, thus generates a very significant reduction in stability. The pK_a associated to the formation of the complexes **5c** and **5e** derived from the **4c** and **4e** are equal to 5.86 and 8.19 respectively, which corresponds to stabilities respectively 130 and 27,500 times lower than that of the complex of the **DNBF**.

The introduction of the CN and CF3 groups on position-6 of the carbocycle of the **DNBF** decreases the stability of the complexes in a less accentuated way. The pK_a related at the complexation of the **4b** is equal to 4.65, which corresponds to a stability of the adduct **5b** only 8 times weaker than that of **DNBF**. As for the adduct, its formation is associated to a pKa of 6.50 which is equivalent to a reduction of stability of a factor 560 compared to complex **1**.

3. Computational details

All calculations were carried out at DFT level using the Gaussian03 program package [15]. All structures were fully optimized and the nature of each stationary point is determined by subsequent frequency calculation at the B3LYP/6- 31G(d)) level of theory [16]. The electronic chemical potential, μ, and the chemical hardness, η, of a substrates were approximated in terms of the one electron energies of the frontier molecular orbitals (FMO) HOMO and LUMO, E_H and E_L, respectively, at the ground state (GS) using [11,17]:

$$\mu = \frac{E_H + E_L}{2} \tag{10}$$

$$\eta = E_L - E_H \tag{11}$$

Starting from the chemical potential and hardness, the global electrophilicity index (ω), measuring the stabilization in energy when a system acquires and additional electronic charge (ΔN) from the environment was defined by Parr as [18]:

$$\omega = \frac{\mu^2}{2\eta} \tag{12}$$

The global maximum charge transfer toward the electrophile was evaluated using [18]:

$$\Delta N_{\max} = -\mu/\eta \tag{13}$$

In order to rationalize the above observed changes in rate constants, calculation of chemical potential and molecular hardness for the electrophile and nucleophile were performed, results are quoted in Table 2.

First of all, qualitatively we can note that all computed electrophilicity of all substrates (between 4.66 and 5.33 eV) are in the range of strong electrophiles within the ω scale [19,20]. Furthermore, the large electrophilicity index computed for the substrates accounts for its facile participation in these addition reactions.

Electrophilicity values of the electrophiles quoted in Table 2 show that **4a** present a higher capacity to attract electrons than **4b**, **4c**, **4d** and **4e**, this result confirms that the presence of SO_2CF_3 group increase the electrophilic

Table 2
Values of chemical potential (μ), molecular hardness (η), electrophilicity (ω).

Molecules	μ (kcal/mol)	η (kcal/mol)	ω (ev)	ΔN_{max}
4a	−136.34	75.69	5.33	1.800
4b	−133.26	73.50	5.25	1.813
4c	−133.02	74.44	5.15	1.786
4d	−128.69	75.88	4.73	1.696
4e	−128.69	77.01	4.66	1.671
H_2O	−71.68	221.80		
DNBF [20]	−136.53	74.00	5.46	

character of the carbocyclic ring of the benzofuroxans structures. Charge transfer seems to explain at least qualitatively the change in the nucleophilic rate constants as a function of the substrate molecule.

Note that, the maximum charges ΔN_{max} that these systems may acquire from the environment consistly decrease with the global electrophilicity power from **4a** to **4e**. The only deceiving point being the ΔN_{max} computed for the **4b** is slightly larger than that of **4a** while experimentally the contrary holds.

Indeed, one can note that the computed electrophilicity of substrate **4a** larger than that of all substrates, thus previewing a reaction kinetically more favorable than that of other substrates.

This fact is further confirmed by the analysis of the chemical potential computed for all substrates. The chemical potential of nucleophile is higher than that of the electrophiles confirming the direction expected for the electronic transfer: from nucleophile with a high chemical potential to an electrophile with a lower chemical potential. The difference of chemical potential among the reacting species $\Delta\mu = \mu_n - \mu_e$ is a measure of electronic transfer, it indicates that reaction substrate **4a** presents a larger electron transfer than reactions with **4b**, **4c**, **4d**, and **4e** substrates, this different behaviour might be at the origin of the differences observed in the rate constant quoted in Table 1 (kinetic study).

On the other hand we can see, when going from **4a** to **4d** the chemical potential increases by 8 kcal/mol, whereas molecular hardness remains quite constant. This indicates that substitution of the CF_3 by SO_2CF_3 group make the system more reactive, this is in agreement with the experimental results. Assuming that the effect of the position of the NO_2, CF_3 or CN groups is not relevant for local or global reactivity, it is interesting to notice that when going from **4b** to **4c** and from **4d** to **4e** molecular hardness remains quite constant and chemical potential increases slightly.

3.1.1. Reactivity–selectivity descriptor

The reactivity–selectivity descriptor $\Delta f(r)$, introduced by Morell et al. [21,22] characterizes the variations of the absolute hardness when the external potential changes, upon, for instance, an approach of reactants during a bimolecular reaction. It is defined as:

$$\Delta f(r) = f^{+}(r) - f^{-}(r)$$

Accordingly, when $\Delta f(r) > 0$ then the point r favours a nucleophilic attack, whereas if $\Delta f(r) < 0$ then the point r favors an electrophilic attack. Therefore, positive values of $\Delta f(r)$ identify electrophilic regions within the molecular topology, whereas negative values of $\Delta f(r)$ define nucleophilic regions. This descriptor has been calculated and the results are shown on (Supplementary data, Fig. S1). Fig. S1 displays, a map of the nucleophilic/electrophilic behaviour of the different sites within the molecule according to the $\Delta f(r)$ descriptor. The regions with $\Delta f(r) > 0$ (red) where a nucleophilic reaction should take place are located in positions ortho and para.

For both substrates 4c and 4e, the regions with $\Delta f(r) > 0$ (red) where a nucleophilic reaction should take place are located in position ortho (C7). For substrates 4a, 4b and 4d the region with $\Delta f(r) > 0$ (red) are located in positions ortho (C5) and para (C7). These results are in perfect agreement with experimental results said, that the NO2 is an electron withdrawing group (EWG) and ortho and para-orienting group and it has been clearly demonstrated in the literature that a para-nitro group plays a leading role in stabilization of the negative charge on σ -anionic complex [1,14].

4. Conclusion

In this work, we have experimentally and theoretically examined the covalent hydration of a serie of nitrobenzofuroxans compounds. Global and local DFT-based reactivity descriptors of the nitrobenzofuroxans substrates have been used to rationalize experimental kinetic data. Chemical potential, molecular hardness and electrophilicity indexes of the reacting species emerge as key elements in the rationalization of experimental rate constants whereas the dual descriptors appears to explain the specific interactions that produce the expected species as product of the chemical reactions under investigation.

5. Experimental

5.1. Rate and pK_a measurements

Stopped-flow determinations were performed on an Applied- Photophysics spectrophotometer, the cell compartment of which was maintained at 25 ± 0.2 °C. Other kinetic and p*K*a determinations were made using a conventional HP8453 spectrophotometer. All kinetic runs were carried out in triplicate under pseudo first-order conditions with a substrates concentration of (3–6) 10^{-5} M.

5.2. Buffers

HCl and KOH solutions were prepared from titrisol. Buffer solutions were made up from the best available commercial grades of reagents. Buffers used were formate (pH 3–4), acetate (pH 4–5.2), succinate (pH 4.8–5.6), cacodylate (pH 5.6–6.8), phosphate (pH 6–7.5), TES (6.9–7.8), tricine (pH 7.8–8.4), bicarbonate (pH 8.47), DABCO (pH 8.50–9.6), CAPS (pH 10.1–10.4).

Acknowledgements

The authors acknowledge the laboratory SIRCOB, University of Versailles, France, for permitting the realization of the experimental part, and also they thanks the Laboratory of Chemical Physics Theory, University Claude Bernard Lyon1, for the realization of the theoretical part of this article.

Appendix A. Supplementary data

Supplementary data associated with this article can be found, in the online version, at http://dx.doi.org/10.1016/j.crci.2012.05.008.

References

[1] F. Terrier, Nucleophilic aromatic displacement. The influence of the nitro group, Wiley-VCH, New York, 1991.
[2] E. Buncel, J.M. Dust, F. Terrier, Chem. Rev. 95 (1995) 2261.
[3] M. Makosza, K. Wojciechowski, Chem. Rev. 104 (2004) 2631.
[4] F. Terrier, F. Millot, W. Norris, J. Am. Chem. Soc. 98 (1976) 5883.
[5] F. Terrier, A.P. Chatrousse, Y. Soudais, M. Hlaibi, J. Org. Chem. 49 (1984) 4176.
[6] F. Terrier, E. Kizilian, J.C. Hallé, E. Buncel, J. Am. Chem. Soc. 114 (1992) 1740.
[7] F. Terrier, M.J. Pouet, J.C. Hallé, S. Hunt, J.R. Jones, E. Buncel, J. Chem. Soc. Perkin Trans. 2 (1993) 1665.
[8] F. Terrier, M.J. Pouet, J.C. Hallé, E. Kizilian, E. Buncel, J. Phys. Org. Chem. 11 (1998) 707.
[9] C.F. Bernasconi, J. Am. Chem. Soc. 92 (1970) 4682.
[10] M. Mokhtari, R. Goumont, J.C. Hallé, F. Terrier, ARKIVOC, (xi) (2002) 168.
[11] (a) R.G. Parr, W. Yang, Density Functional Theory of Atoms and Molecules, Oxford University Press, New York, 1989;
(b) H. Chermette, J. Comput. Chem 20 (1999) 129.
[12] R.G. Pearson, Chemical hardness: application from molecules to solids, Meinheim, Germany, 1997.
[13] H.S. Harned, W.J. Hamer, J. Am. Chem. Soc. 55 (1933) 2194.
[14] F. Terrier, Chem. Rev. 82 (1982) 77.
[15] M.J. Frisch, G.W. Trucks, H.B. Schlegel, G.E. Scuseria, M.A. Robb, J.R. Cheeseman, J.A. Montgomery Jr., T. Vreven, K.N. Kudin, J.C. Burant, J.M. Millam, S.S. Iyengar, J. Tomasi, V. Barone, B. Mennucci, M. Cossi, G. Scalmani, N. Rega, G.A. Petersson, H. Nakatsuji, M. Hada, M. Ehara, K. Toyota, R. Fukuda, J. Hasegawa, M. Ishida, T. Nakajima, Y. Honda, O. Kitao, H. Nakai, M. Klene, X. Li, J.E. Knox, H.P. Hratchian, J.B. Cross, V. Bakken, C. Adamo, J. Jaramillo, R. Gomperts, R.E. Stratmann, O. Yazyev, A.J. Austin, R. Cammi, C. Pomelli, J.W. Ochterski, P.Y. Ayala, K. Morokuma, G.A. Voth, P. Salvador, J.J. Dannenberg, V.G. Zakrzewski, S. Dapprich, A.D. Daniels, M.C. Strain, O. Farkas, D.K. Malick, A.D. Rabuck, K. Raghavachari, J.B. Foresman, J.V. Ortiz, Q. Cui, A.G. Baboul, S. Clifford, J. Cioslowski, B.B. Stefanov, G. Liu, A. Liashenko, P. Piskorz, I. Komaromi, R.L. Martin, D.J. Fox, T. Keith, M.A. Al-Laham, C.Y. Peng, A. Nanayakkara, M. Challacombe, P.M.W. Gill, B. Johnson, W. Chen, M.W. Wong, C. Gonzalez, J.A. Pople, Gaussian 03. Revision B. 05, Wallingford CT, 2004
[16] A.D. Becke, J. Chem. Phys. 98 (1993) 5648.
[17] R.G. Parr, R.G. Pearson, J. Am. Chem. Soc. 105 (1983) 7512.
[18] R.G. Parr, L. Szentpaly, S. Liu, J. Am. Chem. Soc. 121 (1999) 1922.
[19] L.R. Domingo, M.J. Aurell, P. Perez, R. Contreras, Tetrahedron 58 (2002) 4417.
[20] P. Arroyo, M.T. Picher, L.R. Domingo, J. Mol. Struct. 709 (2004) 45.
[21] C. Morell, A. Grand, A. Toro-Labbé, J. Phys. Chem. A. 109 (2005) 205.
[22] C. Morell, A. Grand, A. Toro-Labbé, Chem. Phys. Lett. 425 (2006) 342.